Journal of Ceramic Processing Research. Vol. 15, No. 6, pp. 549~554 (2014)

J O U R N A L O F
Ceramic Processing Research

Tailoring mechanical properties and wettability of nanocrystalline diamond films by control of sp^2/sp^3 bonding ratio

Jong Cheon Park[a], Ok Geun Jeong[a], Sungu Hwang[b], Hee Soo Lee[c], Tae Gyu Kim[d], Jin Kon Kim[d] and Hyun Cho[d]*

[a]*Department of Nano Fusion Technology, Pusan National University, Miryang, Korea*
[b]*Department of Applied Nanoscience, Pusan National University, Miryang, Korea*
[c]*School of Materials Science & Engineering, Pusan National University, Busan, Korea*
[d]*Department of Nanomechatronics Engineering, Pusan National University, Miryang, Korea*

The ratio of sp^2/sp^3 bonded carbon in nanocrystalline diamond (NCD) films was controlled by Ar addition to the CH_4/H_2 mixtures and the effect of the sp^2/sp^3 ratio on the mechanical/tribological properties and wettability was examined. Raman spectroscopy and XPS measurements revealed that Ar addition up to 45 sccm increases the sp^2/sp^3 ratio and induces transition to NCD. Tribological properties such as friction coefficient and wear rate of the NCD film showed a strong dependence on the sp^2/sp^3 bonded carbon ratio while hardness of the NCD films found to be closely related to the sp^3 bond fraction rather than the sp^2/sp^3 ratio. Wettability of the NCD films grown in the $CH_4/H_2/Ar$ microwave plasmas found to be insensitive to the sp^2/sp^3 ratio due to the non-negligible amount of hydrogen on the surfaces.

Key words: Nanocrystalline diamond film, sp^2/sp^3 ratio, Ar addition, Hardness, Friction coefficient, Wettability.

Introduction

Nanocrystalline and ultrananocrystalline diamond (NCD/UNCD) films, nanostructured diamond layers with smooth surfaces grown with a very high nucleation density and a significantly enhanced re-nucleation rate, have attracted much attention due to their exceptional mechanical, physical and chemical properties compared to bulk diamond [1-4]. NCD and UNCD films consist of nanometer-sized sp^3 bonded diamond grains separated by narrow grain boundaries which are the mixture of sp^3 and sp^2 bonded carbon [5]. Their extremely high surface-to-volume ratio provides enhanced multifunctional properties such as high hardness, high elastic modulus, high stiffness, high fracture toughness, high thermal conductivity, chemical inertness, low friction coefficient and high wear resistance. These attributes make them very attractive candidates for a variety of applications including cutting tools, very low friction protective coating, nano/micro-electromechanical systems (NEMS/MEMS) and surface acoustic wave (SAW) devices [6-11].

Tribological properties of diamond films are closely related to sp^2/sp^3 bonded carbon ratio[12]. In general, the increased ratio of sp^2/sp^3 bonded carbon, which indicates increase of lubricious sp^2 hybridization fraction in the film, leads to lower friction coefficient, better wear resistance and reduced internal stresses [13]. NCD and UNCD films are generally grown by microwave plasma enhanced chemical vapor deposition (MPECVD) technique and properties of the grown NCD and UNCD films are dependent on deposition variables such as reactant gas composition, temperature, pressure, pretreatment and seeding process [14-16]. Among these variables, the reactant gas composition plays a significant role in determining the sp^2/sp^3 bonded carbon ratio in the grown NCD and UNCD film. K. Panda *et al*. [17] showed that the sp^2/sp^3 bonded carbon ratio in UNCD film grown in CH_4/Ar mixtures could be increased by N^+ ion implantation and this modification process led to decreased hardness and elastic modulus. They also conducted a comparison study of tribological properties of UNCD and diamond nanorod (DNR) films grown in CH_4/N_2 mixtures and reported that UNCD film showed higher friction coefficient in ambient test atmosphere than nitrogen test atmosphere while DNR film showed opposite tendency [18]. Formation of thin Fe layer on the UNCD film grown in a CH_4/H_2/Ar and subsequent annealing in H_2 atmosphere was found to lead to enhanced sp^2/sp^3 bonded carbon ratio [19].

In this work, we report on the modification of mechanical properties and wettability of NCD films by control of sp^3/sp^2 bonded carbon ratio. NCD films with different sp^3/sp^2 ratios were grown by a cyclic addition of Ar to CH_4/H_2 mixtures during MPECVD, and the effect of sp^3/sp^2 bonded carbon ratio on hardness, friction coefficient and contact angle was examined by X-ray photoelectron spectroscopy (XPS), nanoindenter, scratch tester, and sessile drop method.

*Corresponding author:
Tel : +82-55-350-5286
Fax: +82-55-350-5289
E-mail: hyuncho@pusan.ac.kr

Experimental

NCD films were grown on p-type (100) Si substrates of 2.5×2.5 cm^2. Surfaces of the Si substrates were chemically cleaned in a diluted BOE solution for 1-2 minutes and then washed with acetone and with DI water in ultrasonic bath for 5 minutes, respectively. Surface texturing of Si substrates was performed in SF_6/O_2 inductively coupled plasmas. Subsequently, the substrates were ultrasonically seeded in ethanol suspension of 3-5 nm nanodiamond powders for 30 minutes, followed by ultrasonic cleaning in DI water three consecutive times for 1 minute. Nanocrystalline diamond films were grown in a MPECVD reactor and methane (CH_4) diluted hydrogen was used as the primary reactant gas. The flow rate of CH_4 and H_2 was kept constant at 4 and 200 sccm, respectively, while Ar gas was added cyclically at an interval of 2 sec. The flow rate of Ar was varied from 0 to 60 sccm to examine the effect of Ar concentration on the sp^2/sp^3 bonded carbon ratio. During the deposition, process pressure and microwave power was maintained at 30 Torr and 1000 W, respectively. The substrate temperature controlled by a separate heater was fixed at 700 °C Surface morphology of as-grown NCD films was examined by AFM (PSIA SE100) and FE-SEM (Hitachi S4700). The structural properties of the grown films were characterized by Raman spectroscopy (Thermo Scientific DXR Raman Microscope) and the chemical bonding structure were investigated by X-ray photoelectron spectroscopy (XPS, PHI 5000 VersaProbe) using monochromatic Al-Kα radiation at 1486.74 eV as a probe. Nanoindentation measurements (CSM Instruments, Switzerland) were performed to examine the hardness of as-grown films and the rotational mode of a ball on disk tribometer (CSM Instruments, Switzerland) was used to verify the tribological properties under the condition of test load 3N, sliding distance 200 m.

Results and Discussion

Fig. 1 shows SEM cross-sectional views of NCD films grown for 2 h with variation of Ar content in the reactant gas mixtures from 0 to 60 sccm. The grown films show a granular structure with abrupt grain boundaries, a typical feature of NCD/UNCD films. Columnar growth pattern that is typically observed in the microcrystalline diamond films was not observed. Thickness of the NCD films is in the range of 470-600 nm and deposition rate of NCD film was found to increase as Ar concentration increases up to 45 sccm and then decrease at 60 sccm condition.

Fig. 2 presents Raman spectra of the grown films with different Ar concentrations in the $CH_4/H_2/Ar$ microwave plasmas. The film grown without Ar addition shows distinctive Raman peaks at ~ 1140 cm^{-1}, and ~ 1330 cm^{-1}, suggesting the grown film contains microcrystalline and UNCD diamond phases. The peak at ~ 1330 cm^{-1} is a typical signal of microcrystalline diamond and the peak at ~ 1140 cm^{-1} is attributed to trans-poly-acetylene (TPA) present in abundant grain boundaries between nanoscale diamond grains with general grain size below 10 nm [20, 21]. As Ar concentration in the gas mixtures increases up to 45 sccm, the intensity of the peak at ~ 1140 cm^{-1} increases while the microcrystalline diamond peak at ~ 1330 cm^{-1} decreases, indicating the transition from the mixed phase of microcrystalline and UNCD to UNCD. The film grown with 45 sccm Ar

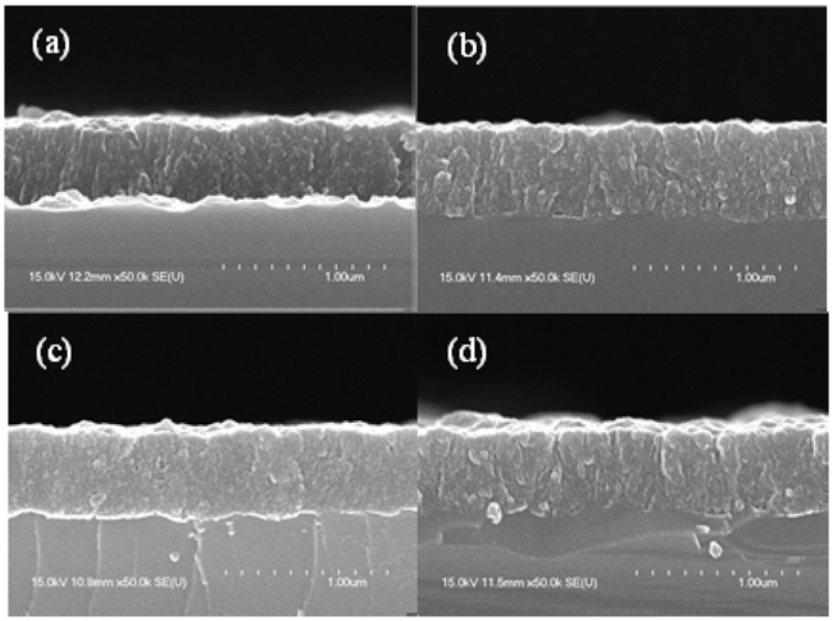

Fig. 1. SEM micrographs of cross-sectional views of the grown NCD films with variation of Ar flow rate in the gas mixtures (a) 15 sccm, (b) 30 sccm, (c) 45 sccm and (d) 60 sccm.

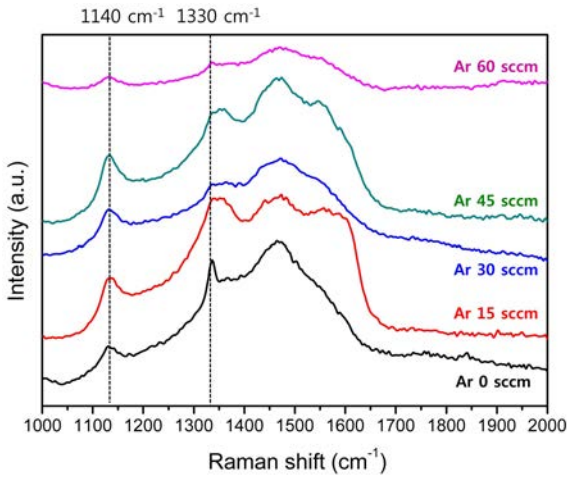

Fig. 2. Raman spectra of as-grown NCD films with variation of Ar flow rate in the gas mixtures; 0, 15, 30, 45 and 60 sccm, respectively.

addition shows the strongest intensity of ~ 1140 cm^{-1} peak while a significant broadening of the peak at ~ 1330 cm^{-1} and evident Raman scattering intensity in the region of 1400-1600 cm^{-1} are observed. It has been reported that broadening of the diamond peak is caused by decreasing the grain size to the nanometer scale, and the development of the graphite band is due to increasing sp^2 bonded carbon at the grain boundaries in the UNCD films [22]. Further increasing the Ar concentration in the gas mixture results in a significant decrease in the intensity for both peaks at ~ 1140 cm^{-1} and ~ 1330 cm^{-1}, most likely due to drastic change in the chemical bonding characteristics.

XPS measurement was performed to examine the effect of Ar addition on the sp^2/sp^3 bonded carbon ratio in the grown NCD films and the XPS C1s spectra of as-grown NCD films are shown in Fig. 3 The data were fitted with Gaussian-Lorentzian peaks with

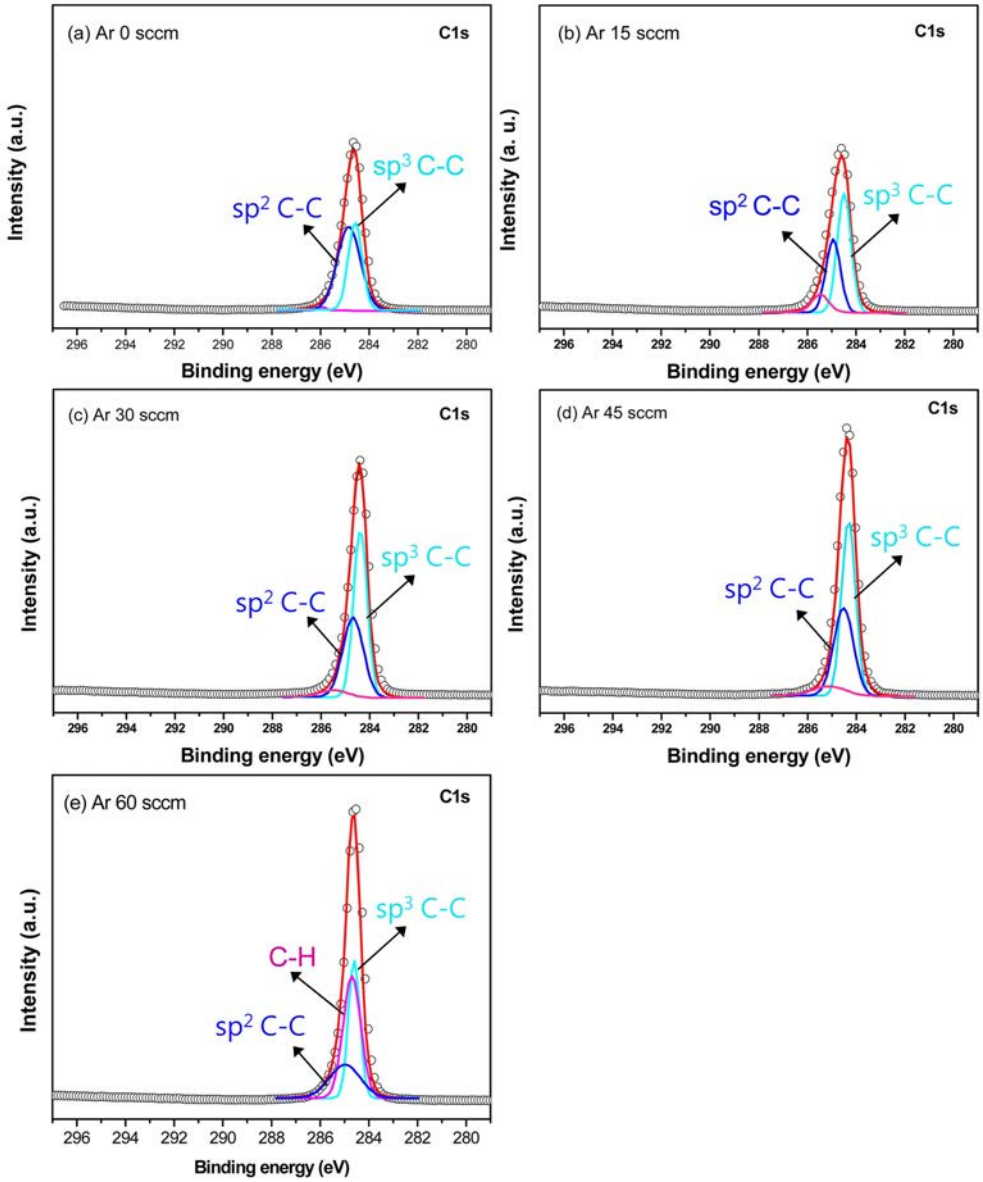

Fig. 3. XPS C1s spectra of the grown NCD films with variation of Ar concentration in the reactant gas mixtures.

Table 1. XPS C1s peaks of NCD films grown with variation of Ar concentration in the gas mixture.

Peak position (eV)	Chemical bonding	Peak intensity (%)				
		Ar 0 sccm	Ar 15 sccm	Ar 30 sccm	Ar 45 sccm	Ar 60 sccm
284.4	sp^2 C = C	37.59	49.48	55.67	56.33	33.04
285.0	sp^3 C-C	59.06	31.48	32.4	33.21	21.09
286.0	C-O	3.35	19.04	11.93	10.46	–

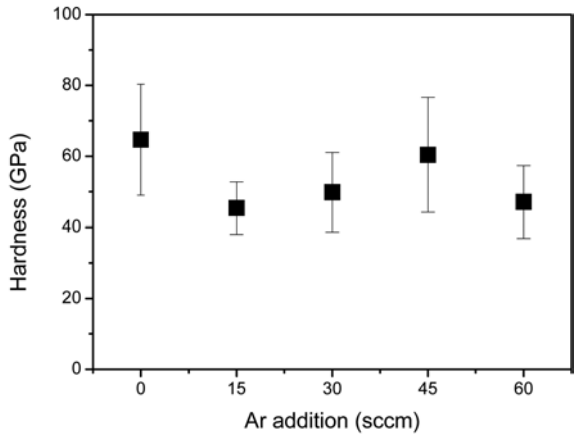

Fig. 4. Hardness of NCD films grown with variation of Ar concentration in the reactant gas mixtures.

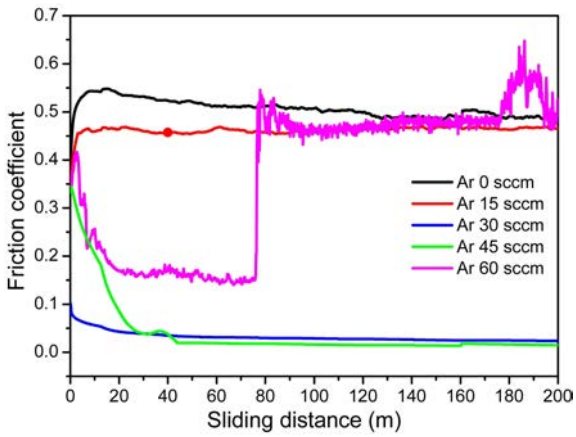

Fig. 5. Friction coefficient of NCD films grown with variation of Ar concentration in the reactant gas mixtures.

binding energies at 284.4, 285, and 286 corresponding to sp^2 C = C, sp^3 C-C, and C-O bonding of the C1s spectra, respectively [17, 18]. The background was subtracted using Shirley's method [23]. Relative intensities of these peaks from the C1s spectra are summarized in Table 1. In the film grown without Ar addition, sp^3 C-C bonding is predominant at 285 eV with a peak intensity of 59.06% and sp^2 C = C bonding present at 284.4 eV with a peak intensity of 37.59%. As Ar is added up to 45 sccm to the reactant gas mixtures, sp^2 C = C peak intensity increases continuously while a significant decrease is observed in sp^3 C-C intensity, indicating the Ar addition induced conversion of sp^3 to sp^2 bonding. This is consistent with the Raman spectroscopy results presented in Fig. 2. The NCD film grown with 45 sccm Ar addition shows the highest sp^2 C = C peak intensity of 56.33 with a sp^2/sp^3 ratio of 1.7. For the film grown with 60 sccm Ar addition, a distinctive peak at 284.7 eV corresponding to C-H bonding appears on the surface. When the Ar concentration in the $CH_4/H_2/Ar$ mixtures exceeds a critical level, surface defects might be formed by enhanced Ar ion bombardment to the surface and this promotes C_2 dimer formation, as reported earlier by Zhou at al. [24]. Then, C-H bond is formed by the reaction between carbon atoms at the defect sites and atomic hydrogen abundantly present in the plasma.

Fig. 4 presents hardness values of NCD films grown with different Ar concentration in the reactant gas mixtures measured by nanoindentation. The film grown without Ar addition produced higher hardness, 65 GPa, than the films grown with Ar addition. As Ar concentration increases to 15, 30, 45 sccm, the average hardness values changes to 45.4, 50, 60.4 GPa, respectively. As described earlier, the sp^2/sp^3 bonded carbon ratio is the key parameter for determining the chemical bond on the NCD surface. However, the hardness of NCD films is known to be closely related to the sp^3 bond fraction rather than the ratio of sp^2/sp^3 bonded carbon [17, 25].

Fig. 5 shows friction coefficients of the NCD films grown with variation of Ar concentration and corresponding wear tract morphologies are shown in Fig. 6. The NCD film grown without Ar addition, with the sp^2/sp^3 bonded carbon ratio of ~ 0.64, shows the friction coefficient of ~ 0.5 and severely deformed film surface with wide wear tracks. This sample showed the highest hardness from nanoindetation measurements as shown in Fig. 4 and is expected to contain high compressive stress, which leads to severe deformation as external stress is applied during the tribology test. Similar behavior is observed for 15 sccm Ar-added NCD film. By sharp contrast, the NCD films grown with 30 and 45 sccm Ar addition, with the sp^2/sp^3 bonded carbon ratio of ~ 1.7, present much lower friction coefficient of ~ 0.024 and ~ 0.016, respectively and much less deformation of the wear track. This result clearly shows that the friction coefficient and wear rate of NCD film is strongly dependent on the sp^2/sp^3 bonded carbon ratio. High sp^2/sp^3 ratio in NCD film provides reduced internal stress which leads to the less deformed surface morphology, resulting in

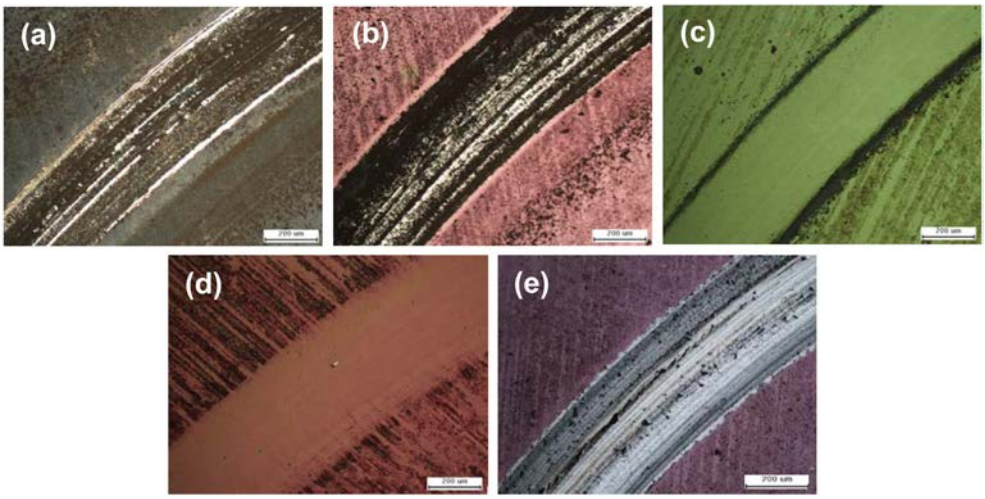

Fig. 6. Optical microscopic images of wear track formed on the NCD films grown with variation of Ar flow rate in the gas mixtures (a) 15 sccm, (b) 30 sccm, (c) 45 sccm and (d) 60 sccm.

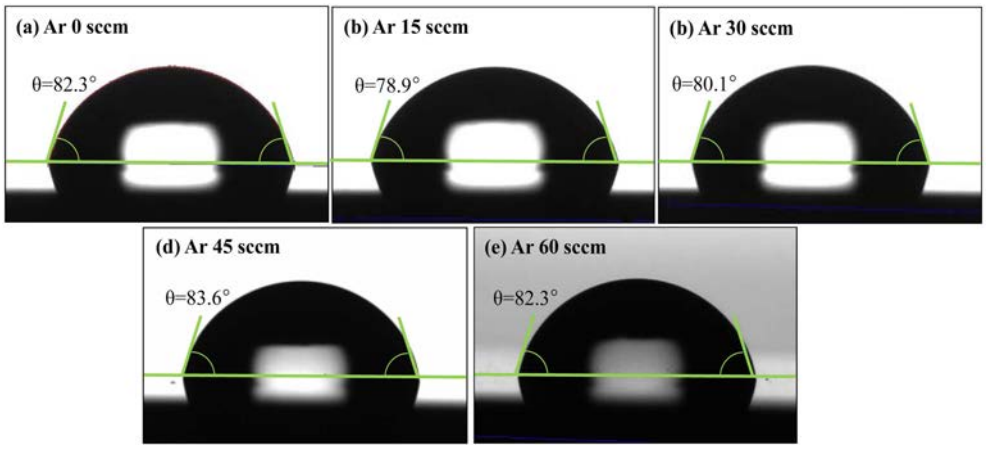

Fig. 7. Contact angle measurements of the NCD films grown with variation of Ar flow rate in the gas mixtures (a) 0 sccm, (b) 15 sccm, (b) 30 sccm, (c) 45 sccm and (d) 60 sccm.

enhanced slip behavior.

Contact angles of the grown NCD films with and without Ar addition to the reactant gas mixtures are shown in Fig. 7. Contact angles around 80° were obtained for all surfaces, which is consistent with previous results reported by other researchers [17, 18], and no noticeable dependence of contact angle on the Ar concentration is observed. In general, wettability of carbon materials is sensitive to the sp^2/sp^3 ratio and hydrogen content on the film surface [26, 27]. In this work, since the NCD films were grown in the CH_4/H_2/Ar microwave plasmas, the grown films are expected to contain non-negligible amount of hydrogen on the surfaces which makes the contact angle insensitive to the sp^2/sp^3 ratio.

Conclusions

Ar was added to the CH_4/H_2 mixtures during the microwave plasma enhanced chemical vapor deposition of NCD films in order to control the sp^2/sp^3 bonded carbon ratio. A significant increase the sp^2/sp^3 bonded carbon ratio, from ~ 0.64 to 1.72, was observed for the NCD films grown with Ar addition. Raman spectroscopy study showed that the intensity of the peak at ~ 1140 cm^{-1} increases while the microcrystalline diamond peak at ~ 1330 cm^{-1} decreases as Ar concentration increases. This result confirms Ar addition induced the transition from the mixed phase of microcrystalline and UNCD to UNCD. XPS measurements also showed that sp^2 C = C peak intensity increases continuously while a significant decrease is observed in sp^3 C-C intensity as Ar is added up to 45 sccm. Hardness of NCD films was found to have a close relationship with the sp^3 bond fraction rather than the sp^2/sp^3 bonded carbon ratio. The friction coefficient and wear rate of NCD film was strongly dependent on the sp^2/sp^3 bonded carbon ratio and the NCD films grown with 30 and 45 sccm Ar addition showed much less deformed surface morphology due to the enhanced slip behavior. The NCD films grown in the CH_4/H_2/Ar microwave plasmas were found not to have Ar concentration dependence of contact angle due to

the non-negligible amount of hydrogen on the surfaces which makes the contact angle insensitive to the sp^2/sp^3 ratio.

Acknowledgments

This work was supported by the national Research Foundation of Korea (NRF) grant funded by the Korea government (MEST) (No. 2012M2B2A9A02030016).

References

1. J. Philip, P. Hess, T. Feygelson, J.E. Butler, S. Chattopadhyay, K.H. Chen and L.C. Chen, J. Appl. Phys. 93 (2003) 2164-2171.
2. O.A. Williams, A. Kriele, J. Hees, M. Wolfer, W. Muller-Sebert and C.E. Nebel, Chem. Phys. Lett. 495 (2010) 84-89.
3. A.V. Sumant, D.S. Grierson, J.E. Gerbi, , J.A. Carlisle, O. Auciello and R.W. Carpick, Phys. Rev. 76 (2007) 235429-235429-11.
4. G. Zilibotti, M.C. Righi and M. Ferrario, Phys. Rev. 79 (2009) 075420-075420-10.
5. A.V. Sumant, D.S. Grierson, J.E. Gerbi, J. Birrell, U.D. Lanke, O. Auciello, J.A. Carlisle and R.W. Carpick. Adv. Mater. 17 (2005) 1039-1045.
6. W.H. Liao, D.H. Wei and C.R. Lin. Nanoscale Res. Lett. 7 (2012) 82-89.
7. D.T. Tran, W.S. Huang, J. Asmussen, T.A. Grotjohn and D.K. Reinhard, New Dia. & Frontier Carbon Technol. 16 (2006) 281-294.
8. P. Bajaj, D. Akin, A. Gupta, D. Sherman, B. Shi, O. Auciello and R. Bashir, Biomed. Devives. 9 (2007) 787-794.
9. N.A. Moldovan, O. Auciello, A.V. Sumant, J.A. Carlisle, R. Divan, D.M. Gruen, A.R. Krauss, D.C. Mancini, A. Jayatissa and J. Tucek, Proc. SPIE. 4557 (2001) 288-298.
10. W. Yang, O. Auciello, J.E. Butler, W. Cal, J.A. Carlisle, J.E. Gerbi, D.M. Gruen, T. Knickerbocker, T.L. Lasseter, J.N. Russell, L.M. Smith and R.J. Hamers, Nat. Mater. 1 (2002) 253-257.
11. A.M. Kovalchenko, J.W. Elam, A. Erdemir, J.A. Carlisle, O. Auciello, J.A. Libera, M.J. Pellin, D.M. Gruen and J.N. Hryn, Wear. 270 (2011) 325-331.
12. D.S. Grierson and R.W. Carpick, 2 (2007) Nanotoday 12-21.
13. A.R. Konicek, D.S. Grierson, P. Gilbert, W.G. Sawyer, A.V. Sumant and R.W. Carpick, Phys. Rev. Lett. 100 (2008) 235502-235502-4.
14. O.A. Williams, O. Douheret, M. Daenen, K. Haenen, E. Osawa and M. Takahashi, Chem. Phys. Lett. 445 (2007) 255-258.
15. D. Zhou, D.M. Gruen, L.C. Qin, T.G. McCauley and A.R. Krauss, J. Appl. Phys. 84 (1998) 1981-1989.
16. H.J. Lee, H.T. Jeon and W.S. Lee, J. Phys.Chem. C. 116 (2012) 9180-9188.
17. K. Panda, N. Kumar, B.K. Panigrahi, S.R. Polaki, B. Sundaravel, S. Dash, A.K. Tyagi and I.N. Lin, Tribology International. 57 (2013) 124-136.
18. K. Panda, N. Kumar, K.J. Sakaran, B.K. Panigrahi, S. Dash, H.C. Chen, I.N. Lin, N.H. Tai and A.K. Tyagi, Surf. Coat. Technol. 207 (2012) 535-545.
19. K. Panda, B. Sundaravel, B.K. Panigrahi, H.C. Chen, P.C. Huang, W.C. Shih, S.C. Lo, L.J. Lin, C.Y. Lee and I.N. Lin, J. Appl. Phys. 113 (2013) 094305-094305-9.
20. P.W. May, M.N.R. Ashfold and Y.A. Mankelevich. J. Appl. Phys. 101 (2007) 053115-053115-9.
21. Y.C. Chu, C.H. Tu, C.P. Liu, Y. Tzeng and O. Auciello, J. Appl. Phys. 112 (2012) 124307-124307-6.
22. D.M. Gruen, A.R. Krauss, C.D. Zuiker, R. Csencsits, L.J. Terminello, J.A. Carlisle, I. Jimenez, D.G.J. Sutherland, D.K. Shuh, W. Tong and F.J. Himpsel. Appl. Phys. Lett. 68 (1996) 1640-1642.
23. V. Janos, Surf. Sci. 563 (2004) 183-190.
24. D. Zhou, D.M. Fruen, L.C. Qin, T.G. McCauley and A.R. Krauss, J. Appl. Phys. 84 (1998) 1981-1989.
25. M. Bai, K. Kato, N. Umehara and Y. Miyake, Thin Solid Films. 377-378 (2000) 138-147.
26. L.Y. Ostrovskaya, A.P. Dementiev, I.I. Kulakova and V.G. Rachenko, Diamond Relat. Mater. 14 (2005) 486-490.
27. A.F. Azevedo, J.T. Matsushima, F.C. Vicentin, M.R. Balden and N.G. Ferreira, Appl. Surf. Sci. 255 (2009) 6565-6570.